The current state of solar modeling

J. Christensen-Dalsgaard, W. Däppen, S. V. Ajukov, E. R. Anderson, H. M. Antia, S. Basu, V. A. Baturin, G. Berthomieu, B. Chaboyer, S. M. Chitre, A. N. Cox, P. Demarque, J. Donatowicz, W. A. Dziembowski, M. Gabriel, D. O. Gough, D. B. Guenther, J. A. Guzik, J. W. Harvey, F. Hill, G. Houdek, C. A. Iglesias, A. G. Kosovichev, J. W. Leibacher, P. Morel, C. R. Proffitt, J. Provost, J. Reiter, E. J. Rhodes Jr, F. J. Rogers, I. W. Roxburgh, M. J. Thompson, R. K. Ulrich

Data from the GONG network and other helioseismic experiments provide a test for models of stellar interiors and for the thermodynamic and radiative properties, on which the models depend, of matter under the extreme conditions found in the Sun. Current models are in agreement with the helioseismic inferences; this result suggests, for example, that the disagreement between the predicted and observed fluxes of neutrinos from the Sun is not caused by errors in the models. However, the GONG data reveal subtle errors in the models, such as an excess in sound speed just beneath the convection zone. This indicates effects that have so far not been correctly accounted for; for example, it is plausible that the sound-speed differences reflect weak mixing in stellar interiors, of potential importance to the overall evolution of stars, and ultimately to estimates of the age of the Galaxy based on stellar evolution calculations.

[J. Christensen-Dalsgaard, S. Basu, Theoretical Astrophysics Center, and Institute of Physics and Astronomy, Aarhus University. W. Däppen, E. J. Rhodes Jr, Department of Physics and Astronomy, University of Southern California. S. V. Ajukov, Sternberg Astronomical Institute, Moscow. E. R. Anderson, J. W. Harvey, F. Hill, J. W. Leibacher, National Solar Observatory, Tucson. H. M. Antia, S. M. Chitre, Tata Institute of Fundamental Research, Bombay. V. A. Baturin, I. W. Roxburgh, M. J. Thompson, Astronomy Unit, Queen Mary and Westfield College, University of London. G. Berthomieu, P. Morel, J. Provost, Observatoire de la Côte d'Azur, Nice. B. Chaboyer, CITA, University of Toronto. A. N. Cox, J. A. Guzik, Los Alamos National Laboratory. P. Demarque, Yale University. J. Donatowicz, G. Houdek, Institut für Astronomie, Universität Wien. W. A. Dziembowski, Copernicus Center, Warsaw. M. Gabriel, Institut d'Astrophysique, Université de Liège. D. O. Gough, Institute of Astronomy, University of Cambridge. D. B. Guenther, Department of Astronomy and Physics, Saint Mary's University. C. A. Iglesias, F. J. Rogers, Lawrence Livermore National Laboratory. A. G. Kosovichev, CSSA, Stanford University. C. R. Proffitt, Computer Sciences Corporation, Goddard Space Flight Center. J. Reiter, Mathematisches Institut, Technische Universität München. R. K. Ulrich, Department of Physics and Astronomy, UCLA.]

Stars are born from contracting interstellar clouds. The initial rapid phases of evolution are rather uncertain; however, the protostar eventually settles down to a state where the forces of gravity and the pressure gradient approximately balance. The continuing contraction releases gravitational energy, which heats up the stellar matter and supplies the luminosity of the early star. Eventually, the temperature in the stellar core gets sufficiently high that the energy released in the fusion of hydrogen into helium begins to contribute to the luminosity. Contraction stops when fusion produces the entire luminosity. The star then enters the very long main-sequence phase, during which essentially all hydrogen in the core is gradually converted into helium. This phase occupies the largest fraction of its life, in the solar case lasting about 10 billion years.

So far, the Sun has used up about half of its hydrogen supply. When hydrogen is exhausted at the center, in about 5 billion years, fusion continues in a shell around the helium core. During this phase the Sun will expand greatly, becoming finally a red giant, which might well swallow the Earth's orbit. The Sun will end as a white dwarf, comprising much of the original mass but with a radius similar to that of the Earth.

In general, a protostellar cloud is likely to be in some state of rotation which is greatly amplified during the contraction phase. The spin-down to the present state of slow solar internal rotation, as helioseismically inferred (*1*), may have involved material motion or instabilities, leading to mixing in the solar interior and thus affecting the structure of the present Sun; the modeling of these processes is currently uncertain, however (*2*).

Modeling the Sun: macro- and microphysics

The details of the description of solar evolution just outlined have been filled in by means of numerical calculations of solar models. When describing the ingredients in such calculations it is convenient to distinguish between "macrophysics" and "microphysics". The latter defines the detailed physical properties of matter in the Sun. Here we discuss the macrophysics, defined as the larger-scale aspects of solar structure, and the assumptions involved in what might be called standard solar modeling (*3*).

The structure of a star is a result of a balance of forces, a balance between the energy loss at the stellar surface and energy generation in the core, and stationary energy transport between the core and the surface. The balance of forces, described as *hydrostatic equilibrium*, provides a relation between the pressure gradient and the gravitational acceleration. The force of gravity is determined by the density distribution in the star: thus we must relate density to pressure (*4*), through the properties of the matter and hence the microphysics. More specifically, the relevant properties of stellar matter are expressed by the equation of state, connecting pressure p, density ρ, temperature T, and composition. The latter is often characterized by the fractional mass abundances X, Y and Z of hydrogen, helium and heavier elements.

The temperature of the stellar interior is determined by energy balance. In much of the Sun, energy transport takes place through radiation and depends on atomic absorption coefficients which determine the *opacity* of stellar matter (*5*). It was also realized early on that radiative transport may require a temperature gradient so steep as to lead to convective instability (*6*): convection then generally dominates the energy transport. In the Sun this occurs in the outer 30 % of the radius (*7*). Due to the efficiency of convective energy transport, it generally requires a temperature gradient only slightly steeper than adiabatic; then pressure and density are approximately related by $p \simeq K\rho^{\gamma_1}$, where K is a constant and $\gamma_1 = (\partial \ln p/\partial \ln \rho)_{\rm ad}$, the derivative corresponding to an adiabatic change, that is, one occurring without heat exchange. The temperature gradient substantially exceeds the adiabatic value only very near the surface (*8*), in a thin region which determines the constant K; in the commonly used mixing-length formalism K is controlled by a parameter that measures convective efficiency (*9*).

In standard solar models it is assumed that the solar luminous output derives from the fusion of hydrogen into helium (*10*). The conservation laws of particle physics dictate that the production of one helium nucleus leads to the emission of two neutrinos. Thus measurements of the flux of neutrinos from the Sun can in principle test the properties of the solar nuclear energy generation. Such measurements have yielded values substantially below those predicted by standard solar models; this is the long-standing solar neutrino problem (*11*).

The life history of the star is intimately related to changes in its composition. These changes can be followed numerically with sequences of models (*12*), starting either during the contraction phase or from an assumed chemically homogeneous initial model. The largest changes in composition result from the fusion of hydrogen into helium. However, changes in the chemical distribution of elements due to gravitational settling also play a significant role in determining the structure of the present Sun (*13*).

A viable model of the present Sun, of solar mass and at the inferred solar age, should have the proper radius and luminosity, as well as the observed surface ratio of heavy elements to hydrogen. These basic properties can be determined fairly accurately. The mass is $M_\odot = 1.989 \times 10^{33}\,\mathrm{g}$, the solar radius is $R_\odot = 6.96 \times 10^{10}\,\mathrm{cm}$, and the solar luminosity is $L_\odot = 3.846 \times 10^{33}\,\mathrm{erg\,s^{-1}}$ (*14*). The chemical composition is known from spectroscopic observations, with the important exception of helium; the present surface abundance yields an abundance ratio between heavy elements and hydrogen of $Z_\mathrm{s}/X_\mathrm{s} = 0.0245 \pm 0.005$ (*15*). The age of the Sun, since the onset of core hydrogen burning, is estimated as $\tau_\odot = (4.52 \pm 0.04)\,\mathrm{Gyr}$ (*16*). The correct values of the radius and luminosity can be obtained in models by adjusting the initial helium abundance and a parameter characterizing the near-surface convection (*17*). Also, the initial heavy-element abundance is generally chosen to obtain the observed surface value in the model of the present Sun.

Given the microphysics, the preceding description provides a well-defined procedure for computing standard models in accordance with the known overall properties of the Sun. On the other hand it involves several significant simplifications, which might compromise the resulting models. It neglects possible macroscopic motion in the solar interior, which would change the composition profile; such motion might result from instabilities associated with the slow-down of rotation or convective overshoot into the stable region beyond the base of the convection zone (*18*). Also, it neglects large convective velocities just below the top of the convection zone that give rise to a turbulent pressure and may contribute up to 10 % of the total pressure (*19*). Finally, it neglects mass variations even though mass loss or accretion may have taken place during the core hydrogen-burning phase of solar evolution (*20*).

The discrepancy between the predicted and measured neutrino fluxes could in principle indicate problems with the standard models. Also, although the solar distribution among the heavy elements is typically similar to the composition of the early solar system as estimated from meteoritic abundances, lithium is underabundant by a factor of about 150 relative to the estimated initial abundance, while beryllium is also somewhat underabundant (*15*). This depletion is likely to have been caused by nuclear burning which, in the case of lithium, requires mixing down to a temperature of around 2.6×10^6 K. Yet in standard solar models the temperature never reaches this value at the base of the convection zone, and the predicted lithium depletion is at most by a factor of 4 (*21*). Thus the observed low lithium abundance is evidence either for mixing well beyond the convection zone at some stage of solar evolution or for mass loss to an extent sufficient to expose depleted material.

In the following we use as reference a standard solar model, Model S, computed with the global parameters mentioned above (*22*).

Some properties of solar oscillations

Models of solar evolution must be checked against observations. The extensive and accurate measurements of the solar five-minute oscillations provide key tests of even subtle features of the models. The solar five-minute oscillations (*23*) consist of a large number of modes that each extend in the radial direction from the surface to the inner *turning point*, whose distance r_t from the solar center is a function of $\nu/(l + 1/2)$, where ν is the frequency and l the degree of the mode. Modes of low degree penetrate almost to the center of the Sun (Fig. 1), whereas higher-degree modes are trapped closer to the solar surface. The modes observed with the GONG network, of degree between 0 and about 250, span a range in r_t between the center and $0.98R$, essentially permitting resolution of solar structure and rotation throughout this range (*1, 24*).

In almost the entire solar interior the thermal time scale is so long, compared with the periods of oscillation, that the oscillations can be regarded as adiabatic. Thus the relative perturbations in pressure and density, when following the motion, are related by

the adiabatic exponent γ_1. To the extent that this relation holds, the oscillations are purely mechanical, with frequencies determined by the variation of p, ρ and γ_1 with radius. The adiabatic approximation breaks down near the surface. Here the full energy equation for the oscillations must be considered, including the perturbation in the radiative, and the highly uncertain perturbation in the convective, flux; thus, although nonadiabatic calculations may indicate the magnitude of the resulting effects on the frequencies, a detailed application to the analysis of the observations is not yet possible (*25*).

Here we consider only adiabatic oscillations and generally treat convection according to the simple mixing-length prescription, neglecting effects of turbulent pressure; then it is straightforward to compute numerically precise frequencies for a given solar model (*26*). Although the approximations undoubtedly introduce errors in the treatment of the model and oscillations in the near-surface region, it is possible to analyze the observed frequencies in a way that largely separates the likely effects of these errors from those of errors in the deeper parts of the model. The near-surface effects on the frequencies have two properties: they depend on frequency because of the detailed nature of the mode in this region; and they depend on the turning-point position, because modes trapped near the surface involve a smaller part of the Sun, and hence are easier to perturb, than modes penetrating to the deep interior. The latter effect can be eliminated by suitable scaling with the mode inertia (*27*). Also, Fig. 1 suggests that near the surface the properties of the modes depend little on degree; so, therefore, does the influence of the near-surface effects (*28*).

Frequency differences (Fig. 2A) between frequencies of models using alternative treatments of the upper part of the convection zone and the normal mixing-length treatment show that the scaled difference is indeed a function of frequency alone. The differences (Fig. 2B) between the GONG mean frequencies and frequencies of the reference Model S largely share the same property. This result confirms that the dominant components in the model errors belong to the near-surface region. Although the nature of the errors is uncertain, their effect has roughly the same magnitude and frequency dependence as those illustrated in Fig. 2A.

A closer look at the frequency differences shown in Fig. 2B reveals a division into two branches, suggesting that there is also a dependence on the depth of penetration of the modes. If one subtracts a smooth function of frequency fitted to the data, and plots the residual against the turning-point radius r_t (Fig. 2C) there is evidently a sharp jump in the residuals at an r_t which corresponds to the region just below the convection zone. Inversion of the frequency differences does indeed reveal a localized sound-speed difference at this point (*24*).

Properties of the solar plasma

The aspects of the microphysics most accessible to helioseismic investigation are the equation of state and opacity. The interior of the Sun is a plasma: it is essentially neutral close to the photosphere, becomes partially ionized in roughly the outer 20000 km, and is nearly fully ionized from there down to the center. The high accuracy of helioseismic data carries the promise of probing the properties of this plasma under conditions that have not yet been achieved experimentally in the laboratory. In the absence of experimental data, solar models are based on theoretical calculations of the equation of state and opacity, which can then be tested against the helioseismic data.

The simplest model is that of a mixture of fully ionized nuclei and electrons obeying the perfect gas law. However, an ideal equation of state can be more general by including deviations from the perfect gas law, due to ionization, radiation and degenerate electrons (*29*). Departures from ideality arise from dynamical interactions between the components of the plasma. One measure of the nonideality is the ratio between the average potential energy resulting from the Coulomb interaction and the kinetic energy of particles (*30*). Although the solar plasma is only slightly nonideal, the deviations from nonideality can be studied in detail because of the observational constraints afforded by helioseismology.

The equation of state

There are two basic approaches to realize nonideal equations of state: the so-called *chemical* and *physical* pictures. In the chemical picture one assumes that the notion of atoms and ions

still makes sense, and ionization is treated like a chemical reaction (*31*). A simple example is the EFF formulation (*32*), which has seen widespread use in stellar modeling. One of the more recent realizations is the Mihalas, Hummer, Däppen (MHD) equation of state, in which modifications of atomic states are expressed in a heuristic and intuitive way, by the probability that the state is occupied as a function of the parameters of the surrounding plasma (*33*).

The physical picture provides a systematic method to include nonideal effects. An example is the equation of state underlying the OPAL opacity project at Livermore (*34*). It starts out from the grand canonical ensemble of a system of the basic constituents (electrons and nuclei), interacting through the Coulomb potential. Configurations corresponding to bound combinations of electrons and nuclei, such as ions, atoms, and molecules, arise in this ensemble naturally as terms in cluster expansions. Any effects of the plasma environment on the internal states are obtained directly from the statistical-mechanical analysis, rather than by assertion as in the chemical picture (*35*).

The first obvious *nonideal* effect is the direct result of the Coulomb force between charged particles. Due to the long-range nature of the Coulomb force, this effect is usually described as a screening of the positive charges by surrounding electrons. It corresponds to an effective attraction between particles. Another nonideal effect is due to the interaction between bound particles and is commonly referred to as pressure (or density) ionization. These nonideal effects have to be included in an equation of state of helioseismic precision. Simple equations of state fail to account for pressure ionization because they usually do not assign a radius to atoms and ions, thus allowing recombination at high densities, such as found, for instance, in the solar center (*36*). Only by treating atoms and ions as extended species can the spurious recombinations be prevented. Even so, a significant fraction of He^+ ions might in principle survive at the solar center (*37*). This could affect solar structure at a level detectable by helioseismology.

Helioseismology may probe important effects of the equation of state through the decrease in γ_1 caused by ionization, particularly in the second ionization zone of helium (lying at a depth of about 15000 km), which is sufficiently deep to be largely unaffected by the

near-surface uncertainties (*38*). Here the response of γ_1 to ionization provides a test of the equation of state and a measure of the helium abundance Y_s in the solar convection zone. Determinations of Y_s are sensitive to uncertainties in the equation of state; recent values tend to be around $Y_s \simeq 0.24$ (*39*).

Helioseismology has clearly shown the effect of the leading-order Coulomb correction in the solar data (*40*). In Fig. 3A the heavy curves show the effect on the model of replacing the EFF equation of state with the MHD formulation. The differences in sound speed are only a few percent; they closely reflect the changes in γ_1 which in turn is intimately linked to the ionization processes in the gas. The resulting frequency differences (Fig. 3B) are huge, compared with the intrinsic accuracy of the observations [*cf.* Fig. 3 of (*41*)]. It is this sensitivity which made immediately obvious the improvements resulting from including the Coulomb effects.

However, beyond the first-order contribution, things become much more subtle. The leading-order correction overestimates the whole Coulomb-pressure effect; at sufficiently high density it causes the total gas pressure to become nonsensically negative. Chemical-picture equations of state, such as MHD, need a switch-off device to prevent negative pressures. In contrast, the OPAL equation equation of state does not suffer from such problems: it contains systematic terms beyond the leading-order Coulomb correction.

The sensitivity of the model and frequencies of going from the MHD to the OPAL equation of state is also illustrated in Fig. 3. The differences are clearly much smaller than for the EFF case, reflecting the fact that both MHD and OPAL contain the leading Coulomb effects. However, the frequency changes are still much higher than the observational uncertainty; although simple inspection of frequency differences between observations and models do not reveal the effects of the equation of state at this level of detail, such effects are quite evident in more sophisticated analyses (*42*). These reveal, for example, that MHD is clearly superior to a simpler formulation involving just the Coulomb correction to the EFF equation of state. Also, there is some evidence from sound-speed inversion that the OPAL equation of state provides a better fit to the Sun than MHD.

Opacity

The opacity of stellar material controls the energy flow through a star, and ultimately its luminosity. Early opacity calculations were based on hydrogenic approximations and related simplifications of the physics (*43*). From the beginning of the 1970s it was noticed that some problems with the calculated properties of variable stars, particularly period ratios of Cepheid stars, could be solved by increasing the interior opacity (*44*). As a result, two new opacity efforts using quite different approaches were undertaken. The OPAL group showed that the earlier opacities grossly underestimated the bound-state contribution to the opacity from iron; the improvements led to the increase of the total opacity required to model Cepheid stars successfully (*45*). Results from the parallel Opacity Project (*46*) are in surprisingly good agreement with OPAL, providing a level of confidence in these new opacities. Introduction of these new opacities has essentially led to the solution of a number of long-standing difficulties in modeling stars and stellar pulsations (*47*), without introducing new problems.

Before the new opacity results were available, it was noted that a modest increase of 10 to 20 % in the opacity just below the bottom of the convection zone could improve the agreement of calculated p-mode frequencies with solar observations (*48*). Such an enhancement in the opacity was obtained by OPAL in this region, mainly as a result of the effect on the ion balance due to an improved equation of state, and led to substantial improvements in the agreement with the helioseismic data (*49*).

The new calculations have increased the opacity for the solar center, causing an increase in the initial helium abundance required to calibrate the model from about 0.24 to about 0.27 (*50*). Interestingly, in models with helium settling this causes a present surface helium abundance of around 0.24, roughly consistent with the helioseismically inferred values (*39*). We also note that there is a recent controversy about collective plasma corrections to the solar-center opacity (*51*).

Progress in solar modeling

In the last decade there have clearly been major efforts directed toward improvements in the physics of the solar interior. To illustrate their effect on models of the Sun, Fig. 4 shows relative differences between models computed with various approximations to the physics and the reference Model S. As discussed in (*24*), the latter model appears to be a relatively good approximation to the sound-speed and density structure of the Sun. Four models are shown, differing in the equation of state and opacity relations, and whether or not gravitational settling was included. It is evident that the MHD equation of state in improves the sound speed in the convection zone. Also, the OPAL opacities substantially improve the structure of the radiative interior, as does including gravitational settling; indeed, it is striking that the latter effect is as large as that due to going from the Cox and Tabor tables to those of OPAL (*52*). To put these difference in perspective, we note that according to the inversions presented in ref. (*24*), c^2 in Model S differs from the Sun by no more than 0.5 %, while the error in the model's density is below 2 %.

Model S shares with other standard solar models predicted fluxes of solar neutrinos substantially in excess of the measured values (*11*). This might suggest that no solution of the neutrino problem can be found by modifying the computation of solar models, while at the same time preserving agreement with the helioseismic data, thus perhaps strengthening the case for a solution involving the properties of the neutrinos (*53*). We note that there are also arguments independent of details of solar models that suggest new physics to be required if the four operating solar neutrino experiments are correct (*54*). It should be realized, however, that helioseismology provides no direct information on the neutrino production which depends primarily on temperature and composition: these quantities are not probed by the oscillation frequencies (*55*).

The close agreement between the structure of the models and that of the Sun has been achieved without any explicit adjustments of the models to match the observations, although much of the improvement in the physics has been motivated by the availability of the highly precise helioseismic data. Rather, the agreement results from incorporating

the best current description of the properties of the solar interior, including gravitational settling. This is a striking demonstration of our ability to model at least the gross features of the interior of a star. It is interesting that the improvements have taken place solely in the microphysics. However, Fig. 2C and the recent GONG results (*24*) clearly demonstrate that there remain subtle differences, indicating the existence of physical effects that have not been taken into account. Although in part these differences arise from remaining inadequacies in the microphysics it is tempting to speculate that we are also seeing effects of errors in the macrophysics and other simplifications of the calculations: a likely candidate is material mixing. Investigation of such effects will require full use of the data from helioseismic experiments such as GONG, combined with a wide range of investigations of properties of other stars. Particularly promising is the emerging possibility of extending seismic investigations to stars other than the Sun (*56*).

References and notes

1. M. J. Thompson *et al.*, this issue [**rotation and dynamics**]

2. Models of the evolution of solar internal rotation assume loss of angular momentum from the convection zone through the solar wind, the coupling to the interior taking place through various types of instability [*e.g.* A. S. Endal and S. Sofia, *Astrophys. J.* **243**, 625 (1981); M. H. Pinsonneault, S. D. Kawaler, S. Sofia, P. Demarque, *Astrophys. J.* **338**, 424 (1989)]. These models have been useful in interpreting rotational velocities and Li abundances in stellar clusters and in field stars near the main sequence. When applied to the Sun, they apparently fail to reproduce the near-uniform rotation of the present solar interior, as inferred from helioseismology [*cf.* Thompson *et al.* (*1*)] indicating that other physical mechanisms must contribute to the solar internal spindown.

3. The notion of "standard" models is an evolving concept; in a loose sense, such models should incorporate the physics which is generally recognized as relevant and for which an adequate theoretical description exists.

4. Simplified stellar models can be based on the condition of hydrostatic equilibrium and the assumption that pressure is related to density alone; for example, J. H. Lane, *Amer. J. Sci. and Arts, 2nd ser.* **50**, 57 (1870); R. Emden, *Gaskugeln* (Teubner, Leipzig, 1907).

5. A substantial breakthrough in the physics of stellar interiors came with the treatment of radiative energy transport. Based on a relation between opacity and temperature gradient, the condition of hydrostatic equilibrium, and the equation of state, one can estimate the luminosity of a star, without regard to the sources of energy. This led A. S. Eddington [*The Internal Constitution of the Stars* (Cambridge University Press, 1926), §169] to consider the possibility that the Sun consists primarily of hydrogen, contrary to the then prevailing view.

6. K. Schwarzschild, *Nachr. Königl. Gesell. Wiss. Gött.* **195**, 41 (1906).

7. From helioseismic inversion the depth of the solar convection zone has been determined to be $(28.7 \pm 0.3)\%$ of the solar radius [J. Christensen-Dalsgaard, D. O. Gough, M. J. Thompson, *Astrophys. J.* **378**, 413 (1991); A. G. Kosovichev and A. V. Fedorova, *Astron. Zh.* **68**, 1015 (1991)].

8. Here the density is so low that convective velocities reaching a considerable fraction of the sound speed are required to sustain the flux of energy.

9. L. Biermann, *Z. Astrophys.* **5**, 117 (1932) and T. G. Cowling, *Mon. Not. R. astr. Soc.* **96**, 42 (1935) were the among the first to use mixing-length treatments to describe the transport of energy by convection. A refined version, now commonly used, was presented by E. Böhm-Vitense, *Z. Astrophys.* **46**, 108 (1958). An alternative more recent formulation is V. Canuto and I. Mazzitelli, *Astrophys. J.* **370**, 295 (1991). Also, hydrodynamical simulations are now able to guide solar modelers [*e.g.* R. F. Stein and Å. Nordlund, *Astrophys. J.* **342**, L95 (1989); N. Brummell, F. Cattaneo, J. Toomre, *Science* **269**, 1370 (1995); Y.-C. Kim, P. A. Fox, S. Sofia, P. Demarque, *Astrophys. J.* **442**, 422, (1995)].

10. Early discussions of hydrogen fusion include C. F. von Weizsäcker, *Phys. Z.* **38**, 176 (1937); G. Gamow, *Phys. Rev.* **53**, 595 (1938); and H. A. Bethe, *Phys. Rev.* **55**, 434 (1939). The details of the processes dominating energy generation in the Sun, in the so-called PP chains, were elucidated by J. B. Oke, *J. Roy. Astron. Soc. Canada* **44**, 135 (1950). Changes in the gravitational and internal energy, resulting from the the fusion-induced changes of solar structure, also make a very small contribution to the luminosity.

11. Neutrinos are detected by radiochemical reactions in ^{37}Cl and ^{71}Ga, and through electron scattering in water, each experiment having a different response to the spectrum of neutrinos emitted by the Sun. The former experiments yield neutrino capture rates of 2.3 and 78 SNU (Solar Neutrino Units, defined as 1 capture per 10^{36} target atoms per second), while the electron scattering experiment yields a flux of the so-called ^{8}B neutrinos of $2.9 \times 10^{6}\,\mathrm{cm}^{-2}\,\mathrm{s}^{-1}$. The corresponding values predicted by Model S discussed below (*22*), which is typical of standard solar models, are 8.2 and 132 SNU, and

$5.9 \times 10^6\,\mathrm{cm}^{-2}\,\mathrm{s}^{-1}$, respectively. For further details on the neutrino problem, see, for example, J. N. Bahcall, *Neutrino Astrophysics* (Cambridge University Press, 1989). A few more recent references are H. Dzitko, S. Turck-Chièze, P. Delbourgo-Salvador, C. Lagrange, *Astrophys. J.* **447**, 428 (1995); and J. N. Bahcall and M. H. Pinsonneault, *Rev. Mod. Phys.* **67**, 781 (1995).

12. Early evolution calculations were carried out by C. B. Haselgrove and F. Hoyle, *Mon. Not. R. astr. Soc.* **116**, 515 (1956), and M. Schwarzschild, R. Howard, R. Härm, *Astrophys. J.* **125**, 233 (1957).

13. Although diffusion and settling were discussed by Eddington [see (*5*)] and are unavoidable consequences of the normal assumptions of stellar modeling, their inclusion in detailed solar models is comparatively recent: see, for example, P. D. Noerdlinger, *Astron. Astrophys.* **57**, 407 (1977); P. Demarque, and D. B. Guenther, *Advances in helio- and asteroseismology: IAU Symposium 123*, J. Christensen-Dalsgaard and S. Frandsen, Eds. (Reidel, Dordrecht, 1988), p. 91; A. N. Cox, J. A. Guzik, R. B. Kidman, *Astrophys. J.* **342**, 1187 (1989); C. R. Proffitt and G. Michaud, *Astrophys. J.* **380**, 238 (1991). The microscopic diffusion and settling rates were discussed by, *e.g.*, G. Michaud and C. R. Proffitt, in *Inside the Stars: IAU Colloquium 137, ASP Conf. Ser.* Vol. **40**, A. Baglin and W. W. Weiss, Eds. (ASP, San Francisco, 1993), p.246; A. A. Thoul, J. N. Bahcall, A. Loeb, *Astrophys. J.* **421**, 828 (1994).

14. The mass is known from planetary motion, and the radius at the level of the visible surface can be measured directly. The solar luminosity is inferred from space-based irradiance measurements, see *e.g.* R. C. Wilson and H. S. Hudson, *Nature* **332**, 810 (1988), assuming isotropic radiation and averaging over the solar-cycle variation of about 0.1 % [for stellar evidence see, *e.g.*, S. Baliunas and R. Jastrow, *Nature* **348**, 520 (1990)].

15. The abundances of elements other than helium can in general be determined with considerable precision. [E. Anders and N. Grevesse, *Geochim. Cosmochim. Acta* **53**, 197 (1989); N. Grevesse and A. Noels, in *Origin and evolution of the elements*, N.

Prantzos, E. Vangioni, M . Cassé, Eds. (Cambridge University Press, 1993), p. 15]. While helium was first detected in the solar spectrum, the formation of the helium lines is so complex that observation gives no precise information about its abundance.

16. The age of the Sun can be estimated from the ages, obtained from radioactive dating, of the oldest meteorites. Wasserburg [in Bahcall and Pinsonneault, *cf.* (*11*)] obtained a meteoritic age of 4.57 ± 0.01 Gyr, while D. B. Guenther, *Astrophys. J.* **339**, 1156 (1989) estimated that hydrogen burning started 40 ± 10 Myr after this time.

17. This calibration was introduced by P. Demarque and J. R. Percy, *Astrophys. J.* **140**, 541 (1964).

18. Rotationally induced mixing was considered by B. Chaboyer, P. Demarque, D. B. Guenther, M. H. Pinsonneault, *Astrophys. J.* **446**, 435 (1995) and by O. Richard, S. Vauclair, C. Charbonnel, W. A. Dziembowski, *Astron. Astrophys.*, in press. Simple models of penetration beneath the convection zone predict a region of nearly adiabatic stratification, followed by a sharp transition to radiative transport [*e.g.* J. H. M. M. Schmitt, R. Rosner, H. U. Bohn, *Astrophys. J.* **282**, 316 (1984); J.-P. Zahn, *Astron. Astrophys.* **252**, 179 (1991)]. The extent of penetration in such simple models has been constrained to a small fraction of a pressure scale height by helioseismic analyses [*e.g.* S. Basu, H. M. Antia, D. Narasimha, *Mon. Not. R. astr. Soc.* **267**, 209 (1994); M. J. P. F. G. Monteiro, J. Christensen-Dalsgaard, M. J. Thompson, *Astron. Astrophys.* **283**, 247 (1994); I. W. Roxburgh and S. V. Vorontsov, *Mon. Not. R. astr. Soc.* **268**, 880, (1994)]. Beyond the region of penetration, which is certainly fully mixed, additional mixing might be caused by gravity waves induced by the penetration.

19. The turbulent pressure is given by $p_{\rm turb} \simeq \overline{\rho w^2}$, where w is the vertical component of the convective velocity, and overbar denotes an average. Mixing-length models with turbulent pressure were computed by N. J. Balmforth, *Mon. Not. R. astr. Soc.* **255**, 603 (1992). Hydrodynamical simulations confirm the importance of $p_{\rm turb}$ in the uppermost parts of the convection zone. Significant uncertainties also arise from the treatment of the convective flux (*9*).

20. A mass loss of $0.1 M_\odot$ during the early parts of the main-sequence phase has been suggested to explain the solar surface Li depletion [*e.g.* A. I. Boothroyd, I.-J. Sackmann, W. A. Fowler, *Astrophys. J.* **377**, 318 (1991); J. A. Guzik and A. N. Cox, *Astrophys. J.* **448**, 905 (1995).

21. See B. Chaboyer, P. Demarque, M. H. Pinsonneault, 1995, *Astrophys. J.* **441**, 865, and references therein. For a review of the solar Li problem, see G. Michaud and P. Charbonneau, *Space Sci. Rev* **57**, 1 (1990)

22. The model used the OPAL equation of state and opacities (*34*). Nuclear reaction parameters were generally obtained from Bahcall and Pinsonneault (*11*). Helium and heavy-element settling was included, using the Michaud and Proffitt coefficients (*13*). The present value of $Z_{\rm s}/X_{\rm s}$ is 0.0245, while the age of the present Sun was assumed to be 4.6 Gyr. The numerical error in the calculation should evidently be substantially smaller than the physical effects which are investigated. The present code has been tested against several other codes, using simplified but precisely defined physics [M. Gabriel, in *Challenges to theories of the structure of moderate-mass stars*, *Lecture Notes in Physics*, Vol. **388**, D. O. Gough, J. Toomre, Eds. (Springer, Heidelberg, 1991), p. 51; J. Christensen-Dalsgaard and J. Reiter, in *GONG '94: Helio- and Astero-seismology from Earth and Space, ASP Conf. Ser.* Vol. **76**, R. K. Ulrich, E. J. Rhodes Jr, W. Däppen, Eds. (ASP, San Francisco, 1995), p. 136]. These and other tests indicate that the numerical error in the models is below 0.005 %.

23. D. O. Gough *et al.*, this issue [**Perspectives** ...]

24. D. O. Gough *et al.*, this issue [**structure inversion**]

25. Nonadiabatic frequency calculations were carried out by, *e.g.*, J. Christensen-Dalsgaard and S. Frandsen, *Solar Phys.* **82**, 165 (1983); A. N. Cox, J. A. Guzik, R. B. Kidman (*13*); N. J. Balmforth, *Mon. Not. R. astr. Soc.* **255**, 632 (1992); and D. B. Guenther, *Astrophys. J.* **422**, 400 (1994). Turbulent pressure and convection introduce additional uncertainties (*19*).

26. J. Christensen-Dalsgaard and D. J. Mullan, *Mon. Not. R. astr. Soc.* **270**, 921 (1994).

27. The mode inertia is defined by $E_{nl} = \int_V \rho |\delta \mathbf{r}|^2 \mathrm{d}V$, where $\delta \mathbf{r}$ is the displacement associated with the oscillation, suitably normalized at the surface, and integration is over the volume V of the star. The frequency change associated with a near-surface modification is proportional to E_{nl}^{-1} [J. Christensen-Dalsgaard and G. Berthomieu, in *Solar interior and atmosphere*, A. N. Cox, W. C. Livingston, M. Matthews, Eds. (Space Science Series, University of Arizona Press, 1991), p. 401].

28. For modes of degree beyond the range covered by the GONG data the l-dependence of the near-surface effects becomes significant. See, for example, D. O. Gough and S. V. Vorontsov, *Mon. Not. R. astr. Soc.* **273**, 573 (1995); H. M. Antia, *Mon. Not. R. astr. Soc.* **274**, 499 (1995).

29. The plasma is still ideal as long as the underlying microphysics does not contain dynamical interactions. The "particles", however, can be be classical or quantum, material or photonic.

30. In the solar interior the ratio between Coulomb and kinetic energy is generally small (typically $\simeq 0.1$), although it reaches about 0.4 in the second helium ionization zone.

31. Such equations of state are based on a model for the free energy of the plasma, incorporating approximate statistical-mechanical models. The ionization equilibria are obtained by searching for the minimum of the free energy under the stoichiometric constraints of the reactions considered. The procedure guarantees thermodynamic consistency.

32. Here the only nonideal effect is a simple prescription to ensure full ionization in stellar cores; see P. P. Eggleton, J. Faulkner, B. P. Flannery, *Astron. Astrophys.* **23**, 325 (1973).

33. D. G. Hummer and D. M. Mihalas, *Astrophys. J.* **331**, 794 (1988); D. M. Mihalas, W. Däppen and D. G. Hummer, *Astrophys. J.* **331**, 815 (1988); W. Däppen, D. M. Mihalas, D. G. Hummer, and B. W. Mihalas, *Astrophys. J.* **332**, 261 (1988).

34. For the OPAL opacity project (Livermore) see C. A. Iglesias and F. J. Rogers, F. J., *Astrophys. J. Lett.* **371**, L73 (1991); F. J. Rogers and C. A. Iglesias, *Astrophys. J.*

Suppl. **401**, 361 (1992). Furthermore, as part of the OPAL project, a physical-picture equation of state was developed that is for the first time suitable for stellar models [F. J. Rogers, *Astrophys. J.* **310**, 723 (1986) and references therein; F. J. Rogers, F. J. Swenson and C. A. Iglesias, *Astrophys. J.* **456**, 902 (1996)]. For more general literature on the physical picture see the book by W. Ebeling, A. Förster, A., V. E. Fortov, V. K. Gryaznov, A. Ya. Polishchuk, *Thermodynamic Properties of Hot Dense Plasmas* (Teubner, Stuttgart, 1991).

35. The physical picture has the power to avoid divergent internal partition functions of bound systems (atoms and ions), a problem that has always plagued the chemical picture.

36. J. Christensen–Dalsgaard and W. Däppen, *Astron. Astrophys. Review* **4**, 267 (1992).

37. Recombination to He^+ ions at the solar center may be allowed. The maximum ratio of He^+ over He^{++} is about 0.30 (*36*). However, there are mechanisms acting to destroy the He^+ ions, and it is possible that helium is virtually fully ionized in the solar core.

38. Obviously, the effect would be even more prominent in the hydrogen ionization zone. However, there the uncertainty in the treatment of convection precludes practical applications.

39. For the helium-abundance determination see S. V. Vorontsov, V. A. Baturin, A. A. Pamyatnykh, *Nature* **349**, 49 (1991); A. G. Kosovichev *et al.*,*Mon. Not. R. astr. Soc.* **259**, 536 (1992); H. M. Antia and S. Basu, *Astrophys. J.* **426**, 801 (1994); A. G. Kosovichev, in *GONG '94: Helio- and Astero-seismology from Earth and Space, ASP Conf. Ser.* Vol. **76**, R. K. Ulrich, E. J. Rhodes Jr, W. Däppen, Eds. (ASP, San Francisco, 1995), p. 89; F. Pérez Hernández and J. Christensen-Dalsgaard *Mon. Not. R. astr. Soc.* **269**, 475 (1994).

40. J. Christensen-Dalsgaard, W. Däppen and Y. Lebreton, *Nature* **336**, 634 (1988); V. A. Baturin, W. Däppen, X. Wang and F. Yang in *Proc. 32nd Liège International Astrophysical Colloquium "Stellar Evolution: What should be done"*, A. Noels, M. Gabriel, N. Grevesse, P. Demarque, Eds. (Université de Liège, 1996), p. 33.

41. F. Hill *et al.*, this issue **[Data products]**

42. See F. Pérez Hernández and J. Christensen-Dalsgaard (*39*). The reason why MHD fits better than EFF plus Coulomb correction is not yet clear. Also, in a similar work S. V. Vorontsov, V. A. Baturin, A. A. Pamyatnykh, *Mon. Not. R. astr. Soc.* **257**, 32 (1992) examined the influence of higher-order Coulomb terms, finding that such terms brought no advantage over the description involving the leading term only. Finally, models computed with the OPAL equation of state appear to provide a better approximation to solar conditions than those using the MHD formulation [A. G. Kosovichev, *Adv. Space Res.* **15**, No.7, 95 (1995); J. Christensen-Dalsgaard, in *Proc. Workshop on Theoretical and Phenomenological Aspects of Underground Physics (TAUP'95), Nucl. Phys. B, Suppl.*, M. Fatas, Ed., in press].

43. A. N. Cox, J. N. Stewart and D. D. Eilers, *Astrophys. J. Suppl.* **11**, 1 (1965); A. N. Cox and J. N. Stewart, *Astrophys. J. Suppl.* **11**, 22 (1965); A. N. Cox and J. N. Stewart, *Astrophys. J. Suppl.* **19**, 243 (1970); A. N. Cox and J. N. Stewart, *Astrophys. J. Suppl.* **19**, 261 (1970); A. N. Cox and J. E. Tabor, *Astrophys. J. Suppl.* **31**, 271 (1976).

44. K. Fricke, R. S. Stobie and P. A. Strittmatter, *Mon. Not. R. astr. Soc.* **154**, 23 (1971); W. B. Stellingwerf, *Astrophys. J.* **83**, 1184 (1978); J. O. Petersen, *Astron. Astrophys.* **34**, 309 (1974); N. R. Simon, *Astrophys. J.* **260**, L87 (1982).

45. The more complete calculations by this group produced factors of up to 100 increase in the opacity of pure iron [C. A. Iglesias and F. J. Rogers, *Astrophys. J.* **371**, L73 (1991); F. J. Rogers and C. A. Iglesias, *Astrophys. J. Suppl.* **79**, 507 (1992); C. A. Iglesias, F. J. Rogers, B. G. Wilson, *Astrophys. J.* **397**, 717 (1992)] at temperatures where transitions originating in the M-shell of iron dominate the absorption. This huge increase in iron opacity is enough to increase the total opacity by a factor of 2-3.

46. The Opacity Project (OP) [see M. J. Seaton, Y. Yan, D. Mihalas and A. K. Pradhan, *Mon. Not. R. astr. Soc.* **266**, 805 (1994); *The Opacity Project*, Vol. **1**, M. J. Seaton, Ed. (Institute of Physics Publishing, London, 1995), and references therein] is mainly an atomic physics effort; plasma effects on occupation numbers are of secondary interest.

47. For example, pulsationally inferred masses [P. Moskalik, J. R. Buchler, A. Marom, *Astrophys. J.* **385**, 685 (1992); S. M. Kanbur and N. R. Simon, *Astrophys. J.* **420**, 880 (1994); J. Christensen–Dalsgaard and J. O. Petersen, *Astron. Astrophys.* **299**, L17 (1995)].

48. See, for example, J. Christensen-Dalsgaard, T. L. Duvall, D. O. Gough, J. W. Harvey and E. J. Rhodes Jr, *Nature* **315**, 378 (1985); S. G. Korzennik and R. K. Ulrich, *Astrophys. J.* **339**, 1144 (1989).

49. Much of the improvement arose because the enhanced opacity increased the depth of the convection zone to match more closely an earlier helioseismic determination (*7*). However, calculations using the new OPAL opacities and the physical-picture equation of state were able to bring the calculated value much closer to the observation [D. B. Guenther, P. Demarque, Y.-C. Kim, and M. H. Pinsonneault, *Astrophys. J.* **387**, 372 (1992); J. N. Bahcall and M. H. Pinsonneault, *Rev. Mod. Phys.* **64**, 885 (1992); J. A. Guzik and A. N. Cox, *Astrophys. J.* **411**, 394 (1993)]. The inclusion of element settling in the models largely explains the residual difference.

50. Simple scaling arguments [see also (*5*)] show that the luminosity is inversely proportional to opacity and increases as a high power of μ. Thus, to compensate for the increase in opacity an increase in μ, and hence in Y, is required [see also V. A. Baturin and S. V. Ajukov, *Astronomy Report* **37**, 489, (1995)].

51. V. N. Tsytovich, R. Bingham, U. de Angelis, A. Forlani, M. R. Occorsio, *Astroparticle Physics*, in press.

52. Such improvement in helioseismic inversion was first noted by J. Christensen-Dalsgaard, C. R. Proffitt, M. J. Thompson, *Astrophys. J.* **403**, L75, (1993).

53. A.G. Kosovichev, in *The Sun and Beyond, 2e Rencontres du Vietnam*, L. M. Celnikier, Ed. (Editions Frontières: Gif sur Yvette), in press. For a recent review see R. S. Raghavan, *Science* **267**, 45 (1995).

54. J. N. Bahcall, H. A. Bethe, *Phys. Rev. Lett.* **65**, 2233 (1990); J. N. Bahcall, *Phys. Lett. B* **33k**, 276 (1994).

55. The helioseismic inferences constrain the solar pressure, density and sound speed. With no further constraints, this leaves considerable freedom for the temperature and composition profile and hence for the neutrinos. Note, for example, that for a fully ionized ideal gas $c^2 \propto T/\mu$; hence T/μ is constrained but not T and μ separately; see H. M. Antia and S. M. Chitre, *Astrophys. J.* **442**, 434 (1995). Models can be found which agree with both the helioseismic data and the ^{37}Cl neutrino detections. However, in such models the internal opacity would have to be essentially zero.

56. T. M. Brown, *Ann. Rev. Astron. Astrophys.* **32**, 37 (1994).

57. D. O. Gough and J. Toomre, *Ann. Rev. Astron. Astrophys.* **29**, 627 (1991).

58. S. Basu and H. M. Antia, *J. Astrophys. Astron.* **15**, 143 (1994). Convection was treated using the Canuto and Mazzitelli formulation [see (*9*)].

59. A. G. Kosovichev, in *Proc. Fourth SOHO Workshop: Helioseismology*, J. T. Hoeksema, V. Domingo, B. Fleck, B. Battrick, Eds. (ESTEC, Noordwijk, ESA SP-376, Vol. **1**, 1995), p.165.

60. C. S. Rosenthal *et al.*, in *Proc. Fourth SOHO Workshop: Helioseismology*, J. T. Hoeksema, V. Domingo, B. Fleck, B. Battrick, Eds. (ESTEC, Noordwijk, ESA SP-376, Vol. **2**, 1995), p.459.

61. We thank Regner Trampedach for assistance with the graphics. The work reported here was supported in part by the Danish National Research Foundation through the establishment of the Theoretical Astrophysics Center, and in part by the grant AST-9315112 of the National Science Foundation. This work utilizes data obtained by the Global Oscillation Network Group (GONG) project, managed by the National Solar Observatory, a Division of the National Optical Astronomy Observatories, which is operated by AURA, Inc. under a cooperative agreement with the National Science Foundation. The data were acquired by instruments operated by the Big Bear Solar Observatory, High Altitude Observatory, Learmonth Solar Observatory, Udaipur Solar Observatory, Instituto de Astrofísica de Canarias, and Cerro Tololo Interamerican Observatory.

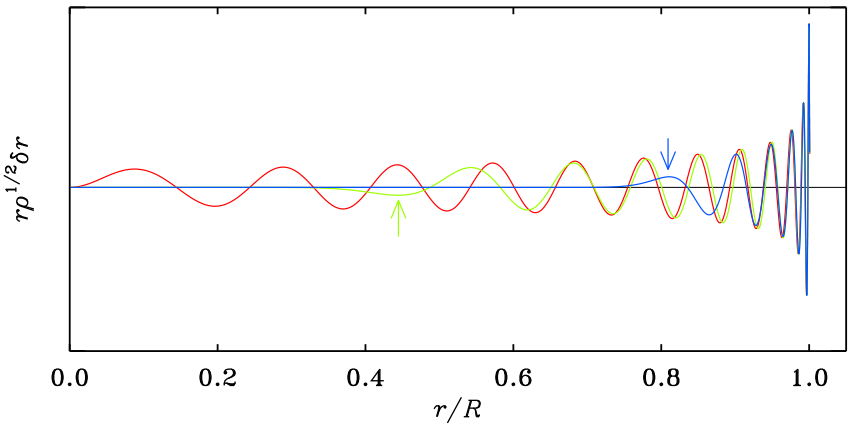

Fig. 1

Radial variation of the eigenfunction for three modes of similar frequency but differing degree l. The red curve shows a mode of degree $l = 0$ and frequency $\nu = 3310\,\mu$Hz, the green curve is for $l = 20$, $\nu = 3375\,\mu$Hz and the blue curve is for $l = 70$, $\nu = 3405\,\mu$Hz. The quantity plotted reflects the distribution of energy in the modes and hence their sensitivity to solar structure. The arrows indicate the locations $r_{\rm t}$ of the asymptotic turning points, determined by the frequency ν and l from the relation $c(r_{\rm t})/r_{\rm t} = 2\pi\nu/(l+1/2)$ (*57*), c being the adiabatic sound speed.

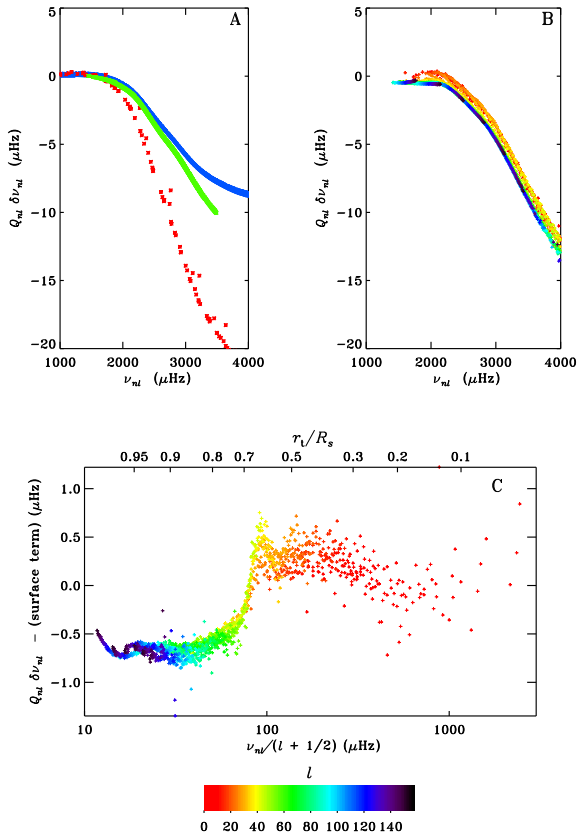

Fig. 2

Frequency differences scaled by $Q_{nl} = E_{nl}/\overline{E}_0(\nu_{nl})$, where $\overline{E}_0(\nu)$ is the inertia of radial modes, interpolated to the frequency ν (*27*). As argued in the text, any contribution to such scaled differences coming from errors in the near-surface region would be expected to depend primarily on frequency. (A) Differences for three modifications of the near-surface region of solar models, relative to a normal mixing-length model: the blue points result from using an alternative treatment of the convective flux (*58*); the green points are based on inclusion of turbulent pressure in the mixing-length treatment (*59*); and for the red points the uppermost parts of the convection zone were represented by an averaged hydrodynamical simulation (*60*). (B) Differences between GONG observed frequencies and frequencies of the reference Model S. (C) Differences in panel (B), after subtracting a smooth fit to the frequency-dependent component. The residuals have been plotted against $\nu/(l+1/2)$ (lower abscissa) which is directly related to the turning-point radius r_t of the mode (upper abscissa). In panels B and C the degree l has been coded in color, according to the color bar shown at the bottom of the figure.

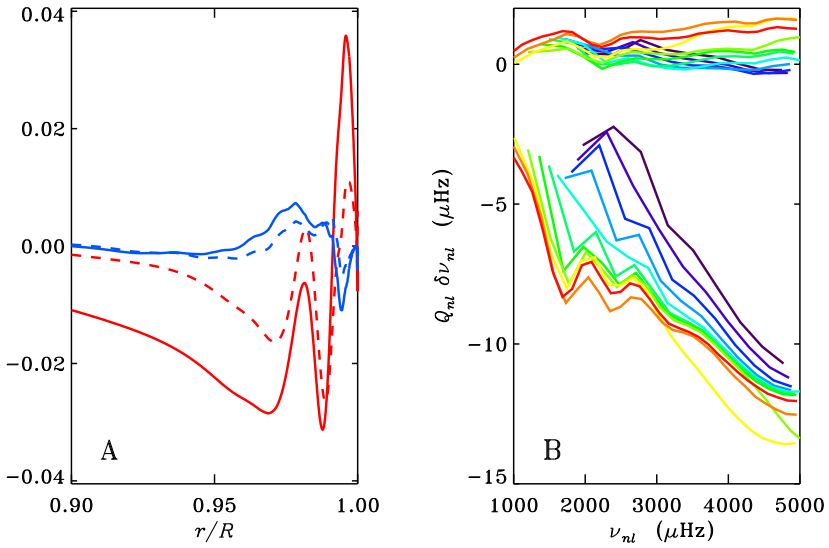

Fig. 3

Panel (A) shows relative differences, at fixed radius, in γ_1 (dashed curves) and squared sound speed (continuous curves) between two pairs of models: the red lines are for a model computed with the EFF equation of state (*32*) minus a model computed with the MHD formulation (*33*); the blue lines are for differences between a model computed with the OPAL equation of state (*34*) and the MHD model. Panel (B) shows corresponding frequency differences between the EFF and MHD models (lower set of curves) and the OPAL and MHD models (upper set of curves), for modes of degree $0, 20, \ldots, 200$. Points of the same degree have been connected by lines coded in color according to l as in Fig. 2.

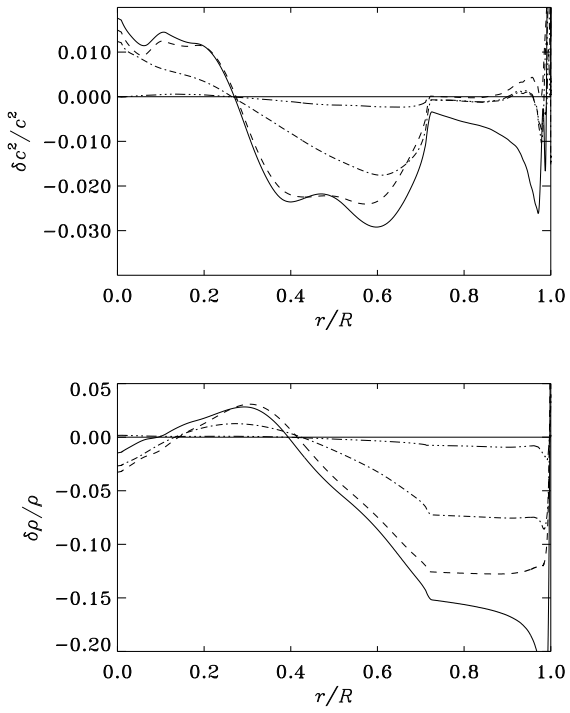

Fig. 4

Differences, relative to the reference Model S of squared sound speed c^2 and density ρ in four models based on various approximations to the physics. The following line styles are shown: Solid lines: EFF equation of state (*32*), Cox and Tabor opacities (*43*); dashed lines: MHD equation of state (*33*), Cox and Tabor opacities; dot-dashed lines: MHD equation of state, OPAL opacities (*34*); triple-dot-dashed lines: the same, but including settling of helium and heavy elements.